INNOVATIONS IN MEDICAL PHYSICS

APPLICATIONS AND TECHNOLOGY

THE DEVELOPMENT OF MODERN TIME-RESOLVED ANGIOGRAPHIC IMAGING; APPLICATIONS OF UNDERSAMPLED ACQUISITION AND CONSTRAINED RECONSTRUCTION

Charles A Mistretta

The University of Wisconsin-Madison-USA, Departments of Medical Physics, Radiology and Biomedical Engineering

Abstract—Prior to the introduction of DSA, time-resolved X-ray angiography required film changers and darkrooms and provided an awkward mechanism for interventional radiology. DSA stimulated the development of the field of interventional radiology providing greater convenience and safety. Time resolved angiography was then extended to MRA using undersampled acquisition techniques such as TRICKS and VIPR. This was followed by the development of constrained reconstruction such as HYPR which, when combined with VIPR, provided undersampling factors of 800 relative to the traditional Nyquist requirements. The HYPR concept was subsequently applied to a broad range of medical imaging applications often offering an order of magnitude improvement in dose or acquisition speed. The success of the concepts of underampling and constrained reconstruction has led to what has been referred to as the Post-Nyquist Era of medical imaging. The concept of undersampling has recently been extended to DSA which now includes a non–time-resolved 3D DSA capability using rotational C-arm acquisition and cone beam reconstruction. By modifying the acquisition to include time-dependent projection information, it has been possible to develop 4D DSA which provides time-resolved DSA volumes up to 300 times faster than with sequential C-arm rotations. Relative to CTA, which requires exposure for each time frame, 4D DSA obtains up to 300 time-resolved volumes following a single C-arm rotation and a single contrast injection. Using similar ideas, 4D Fluoroscopy is under development and will provide a new interventional capability by providing views previously unobtainable due to C-arm geometrical constraints. This promises to increase the speed and safety of interventional procedures. The extension of undersampled acquisition and constrained reconstruction using iterative reconstruction techniques promises to further extend the possibilities for angiographic as well as other medical imaging applications.

Keywords— angiography, time-resolved, constrained reconstruction, undersampled acquisition, 4D DSA

INTRODUCTION

This article will trace the history of the development of modern angiographic imaging techniques beginning with X-ray DSA then continuing with time resolved MRA and then returning to the current version of DSA that now provides full 4D capabilities. Many groups have made important contributions to this process and we confess in advance that this article will be heavily influenced by our own recollections and may overemphasize the work with which we are most familiar.

The first angiogram in a human patient was obtained by Egas Moniz using a direct needle injection into the carotid artery [1]. The isolation of the vasculature was greatly improved by the introduction of film subtraction angiography by Ziedses des Plantes [2] who quite amazingly introduced this concept and the concept of tomography in the same PhD dissertation in 1934. The concept of subtraction is one that pervades all future developments in MRA and DSA. An illustration of Ziedses des Plantes film subtraction technique is shown in Figure 1.

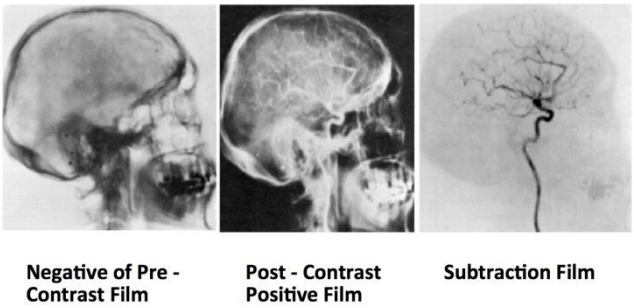

Figure 1. Illustration of Ziedses des Plantes film subtraction technique.

Film subtraction angiography was commonly used for interventional procedures, which relied on rapid film changers, and required devices to be left in the patient while films were processed in a darkroom.

Film subtraction angiography remained the standard well into the 1970s where excellent image quality was obtained but remained time consuming and ill-suited to real time intervention.

Generalized Subtraction Imaging

$$I(x, y,z,E,t) - I(x + \Delta x, y + \Delta y,z + \Delta z,E + \Delta E,t + \Delta t) =$$

$(dI/dx)^* \Delta x + (dI/dy)^* \Delta y$	2D spatial processing
$+(dI/dE)^* \Delta E +$	Dual energy
$+(dI/dt)\, \Delta t +$	DSA
$+(dI/dz)\, \Delta z$	Tomography/CT
$+(d^2I/dEdz)\Delta E \Delta t$	Dual energy CT
$+ (d^2I/dEdt)\, \Delta E \Delta t$	Dual energy DSA
$+ (d^2I/dzdt)\Delta z \Delta t$	CTA, 4D DSA
$+ (d^3I/dEdzdt)\, \Delta E \Delta t \Delta z$	Dual energy 4D DSA

Figure 2. Taylor series expansion showing potential imaging modalities obtainable using X-rays.

In 1973 we discussed the concept of generalized subtraction imaging [3] and described the various potential imaging modalities that might be implemented using first, second and third order image subtraction involving differences in the spatial variables, energy and time. The imaging modalities categorized in this way are shown in Figure 2.

The terms in Figure 2 did not describe how the various modalities could be implemented and for example, certainly did not describe CT or DSA. However, with our recent demonstration of the feasibility of dual energy 4D DSA, essentially all of the modalities predicted by the terms in Figure 2 have now been implemented.

During the early 1970s our group at the University of Wisconsin was concerned with dual energy imaging (the dI/dE term) [4]. We were using quasi-monoenergetic x-ray spectra, which peaked above and below the k-edge of iodine as shown in Figure 3.

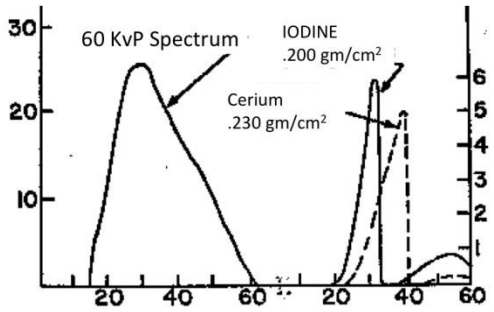

Figure 3. Formation of quasi-monoenergetic beams using filtration.

The idea for dual energy imaging was to perform a weighted subtraction of images formed from the two spectra in order to cancel bone or tissue and isolate iodine. Initially the subtraction was performed using a series of two silicon target storage tubes, the first that performed a difference image and the second that integrated the results [5]. The sensitivity of the subtraction apparatus is illustrated in our first subtraction experiment that consisted of a periodic insertion of a tongue depressor and piece of paper into the imaging field. This is illustrated in Figure 4.

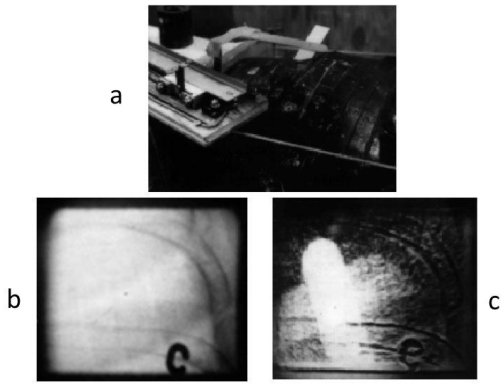

Figure 4. Enhancement of periodic x-ray contrast using dual storage tube apparatus. Figure 3a shows the apparatus. 3b shows the unsubtracted image. 3C shows the integrated subtraction result.

The storage tube apparatus was used to image periodic contrasts produced by a rotating filter that generated the spectra shown in Figure 3

Although the method was sensitive to small amounts of iodine, it required the careful balancing of several analog parameters to achieve the correct subtraction weighting. Because of this, X-ray exposures had to be repeated frequently.

Just prior to the development of DSA the group at Toulouse [6] reported excellent film subtraction results using intravenous injections and improved film techniques as shown in Figure 5

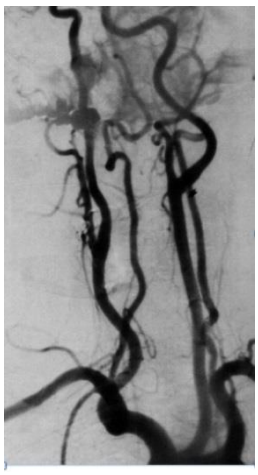

Figure 5. Intravenous film subtraction angiography-Ducos de Lahitte et al. 1979.

About the same time Ovitt, Nudelman, Capp and others at the University of Arizona [7] and Brennecke and Heintzen from the Kiel Kinderklinic [8] reported off-line digital processing of angiograms using time subtraction. Their early results are shown in Figures 6 and Figure 7.

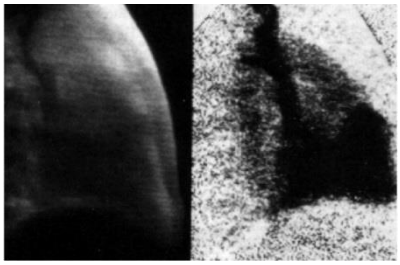

Figure 6. Subtracted pediatric left ventriculogram from Brennecke and Heintzen, 1976.

Figure 7. Offline digital subtraction angiograms showing pre-injection (upper left), post injection (upper right), subtraction lower left) and enhanced subtraction (lower right) From Ovitt et al, 1977.

Figure 8. Real time DSA. University of Wisconsin, 1978.

These results inspired our group to modify our dual energy real time digital processor to facilitate implementation of time subtraction angiography [9-13]. An early result is shown in Figure 8.

At the time of the commercial introduction of DSA at the Dallas RSNA in 1980, it was hoped that all diagnostic angiography could be done using DSA with intravenous injections. Within two years there were thirty companies manufacturing DSA equipment. However, it soon became evident that due to artery/vein overlap and limited signal to noise ratio more consistent results were obtained when the real time DSA apparatus was used with arterial injections. These injections were now possible with smaller catheters and smaller iodine doses than used with film angiography. Complication rates rapidly decreased using the new DSA technique that greatly facilitated the development of interventional radiology [14].

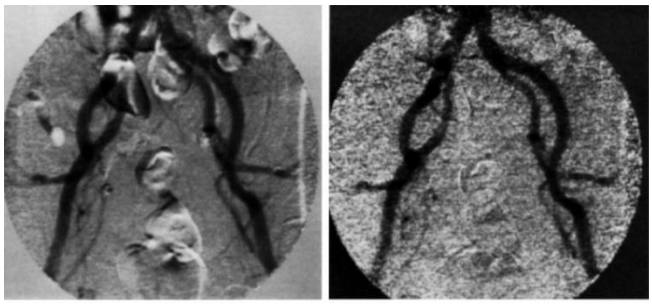

Figure 9. Comparison of time subtraction DSA and hybrid energy/time subtraction DSA

We briefly considered another generalized image subtraction term called hybrid energy/time subtraction ($d^2I/dEdt$) and incorrectly reasoned that since the temporal subtraction would remove non-vascular anatomy, there was no need for energy subtraction. However it was recognized by Brody[15] that this method could be used as a means of removing soft tissue artifacts from DSA exams in which soft tissue swallowing artifacts or misregistration due to bowel peristalsis could degrade image quality. This mode was subsequently introduced commercially but was eventually abandoned due to the poor signal to noise ratio obtained with the second order subtraction. An example of energy/time subtraction is shown in Figure 9.

It is interesting to note that with the improved SNR provided by the constrained reconstruction techniques as well as the arbitrary views permitted by the 4D DSA technique that will be described later, the most significant problems of these early intravenous techniques have been overcome.

The origin of the constrained reconstruction and undersampled acquisition techniques that made 4D DSA possible were initially developed within the context of our studies in MR angiography.

MAGNETIC RESONANCE ANGIOGRAPHY

In 1993 Prince [16] introduced the gadolinium-enhanced MRA method. Although excellent 3D images could be obtained with intravenous gadolinium injections, the timing of the data acquisition was a major problem. If the central portions of k-space were obtained prior to or after peak arterial opacification there could be significant problems with signal dropout or venous contamination in the single image volumes that were typically acquired in a time of about 30 seconds. Additionally, the single image acquisition techniques did not provide dynamic information.

Several methods were developed to try to time the data acquisition. These included the use of test boluses [17], region of interest signal detection [18], and the use of 2D MR fluoroscopy [19, 20]. Because peak opacification of various vessels may occur at different points in time, none of these methods were completely satisfactory.

Attempts to obtain dynamic image series in MRA were done using Keyhole imaging [21] in which the central portion of k-space was repeatedly acquired and combined with high spatial frequency information acquired at the end of the examination. While this provided some sense of the vascular dynamics, high spatial frequency information was prematurely displayed throughout the examination. Several investigators had been exploring variable rate k-space sampling in non-contrast-enhanced MRA applications [22]. We applied these principles to MRA in the TRICKS method (time resolved imaging of contrast kinetics) in 1996 [23,24]. In this technique, during the passage of the contrast material, data from the center of k-space were acquired alternately with data from the peripheral regions of k-space so that there was a new central k-space contrast weighting for each of several time frames as in keyhole imaging. However after several central k-space samples were obtained there would be a new complete sampling of outer k-space. This resulted in an acceleration factor of four relative to the conventional static examination and provided central k-space sampling throughout the bolus, reducing the need to carefully time the acquisition relative to the contrast arrival.

Figure 10 shows an early TRICKS examination that clearly showed the passage of contrast through the cerebral vasculature. Although spatial and temporal resolution were limited by the use of conventional Cartesian acquisition and the time consuming phase

encoding process, TRICKS represented a significant MRA breakthrough and thirteen years after its introduction remains the most widely used technique for time resolved MRA.

In an effort to achieve greater degree of acceleration relative to the traditional acquisitions prescribed to obey the Nyquist theorem we began to investigate the use of radial k-space acquisition, the technique originally used by Lauterbur. The radial approach had been abandoned in favor of Cartesian acquisition because of gradient imperfections that made it difficult to pass through the center of k-space on each acquisition and a fifty percent increase in the number of acquisitions relative to Cartesian acquisition required to satisfy the Nyquist theorem.

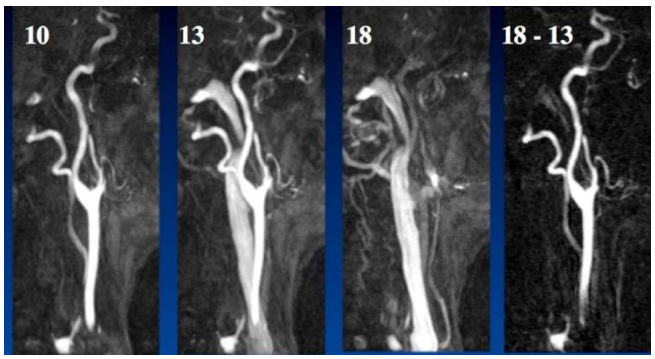

Figure 10. TRICKS examination showing time frames 10, 13 and 18. On the right frame 18 containing the jugular vein has been subtracted for frame 13 to isolate the arterial phase.

Scheffler and Hennig [25] demonstrated that radial acquisition could be used for small field of view imaging and demonstrated that in radial acquisition, when angular undersampling was done, the point spread function maintained high resolution in the central portion but showed radial streak artifacts in the peripheral regions. The size of the adequately supported small field of view decreased with the amount of angular undersampling.

In 2000 our laboratory began its study of radially acquired MRA. This was motivated by our desire to speed up the MRA acquisition by eliminating the time consuming phase- encoding process associated with Cartesian imaging. Peters [26] investigated the use of radial sampling in 2D and found that for the purposes of full field-of-view angiography a factor of four undersampling could be used with tolerable artifacts. For the same acquisition time as Cartesian a factor of four resolution increase was realized in the phase encoding direction.

We then realized that if undersampling were performed in a 3D acquisition, the artifacts would have a full 3D angular range in which to disperse. We implemented a technique called VIPR [27] (vastly undersampled imaging with projections) and found that excellent MR angiograms could be achieved with a factor of about 30 violation of the Nyquist theorem. Figure 11 shows the VIPR k-space acquisition consisting of radial projections all passing through the center of k-space and an early VIPR examination using a phase contrast pulse sequence (PC VIPR). Note the absence of significant artifacts.

PC VIPR permits voxel sizes an order of magnitude smaller than can be achieved in the same time as with Cartesian acquisition. This has permitted the measurement of pressure gradients using the Navier-Stokes equations, estimates of wall shear stress and, when implemented with cardiac gating, has provided dynamic flow information that can be viewed from arbitrary angles greatly simplifying applications such as those used pediatric cardiology [28-32].

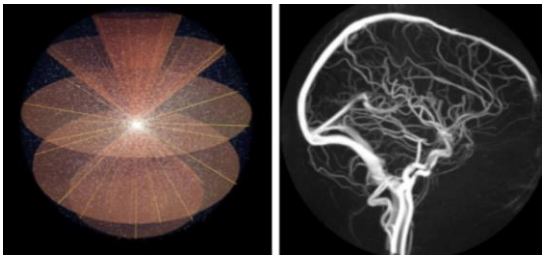

Figure 11. VIPR k-space trajectory and an early PC VIPR examination using an undersampling factor of 36.

Another significant advance in connection with accelerated MRA was the application of constrained reconstruction techniques to reduce undersampling artifacts and to increase SNR. Constrained reconstruction had been reported in MR by Lauterbur's group as early in 1993 [33]. This and the more recent KT-Blast and KT-Sense techniques [34] used the idea of a training image to constrain the reconstruction of time frames. While at the 2006 ISMRM meeting, during the process of thinking about training images we heard a plenary lecture by Jeurgen Hennig in which he reminded us that if the vessel configuration were known in advance and the vessel filling proceeded according to a well defined contrast curve, a complete 4D angiographic reconstruction could be performed by acquiring a single k-space point or single projection for each time frame.

We began to wonder how many projections would be required if the situation were not quite the same as in the Hennig example. We began to imagine a training image depicting the eligible vascular voxels and single projection information being backprojected and deposited only in the predefined vascular space. This constrained back projection was significantly different from

conventional filtered back projection used for CT reconstruction. We found that a surprisingly small number of projections were required to obtain highly accelerated dynamic MRA sequences. This approach was called HYPR for "highly constrained back projection" [35].

An improved version of HYPR that limits the deposition of information to the local region in which it belongs is called HYPR-LR [36]. In this method a composite constraining image is formed from a series of undersampled time frame acquisitions in which the projection angles are interleaved. For a long acquisition this results in a fairly well sampled composite image that can be used to constrain the reconstruction of individual time frames. The individual time frame data are convolved to provide a series of temporal weighting images. These are multiplied by the constraining image resulting in a time frame having nearly the same SNR as the constraining image and nearly the full resolution of the constraining image even though the resolution and SNR associated with the acquired time frame data would be limited. This sort of approach woud have provided adequate SNR for the old hybrid X-ray time/energy approach shown in Figure 9.

Figure 12 shows time resolved MRA frames acquired using a 2D Stack of Stars geometry in which radial imaging is used in-plane and one dimension of phase encoding is used in the slice direction. These are compared to conventional filtered back projection. In spite of an acceleration factor of 50, the HYPR images are far cleaner. Sixteen projections instead of the Nyquist designated 800 projections were used.

The combination of VIPR and HYPR have led to acceleration factors as large as 800 [37] as illustrated in Figure 13. In this application called Hybrid HYPR/VIPR MRA the composite image is formed in a separately acquired examination, typically lasting a few minutes. In Figure 13 the composite was formed with PC VIPR and was used to constrain the reonstruction of highly undersampled VIPR time frames. Again, the SNR and spatial resolution of the composite image is transferred to the time frames. This approach greatly reduces the traditional tradeoff between spatial and temporal resolution.

Compressed sensing can add modest acceleration factors by removing streaks in undersampled acquisitions and can be used in conjunction with more highly accelerated techniques like Hybrid HYPR VIPR. Parallel imaging has been used to accelerate the TRICKS techniques and the use of 2D parallel imaging has been used to facilitate accelerations on the order of 40 in the Cartesian CAPR technique [38].

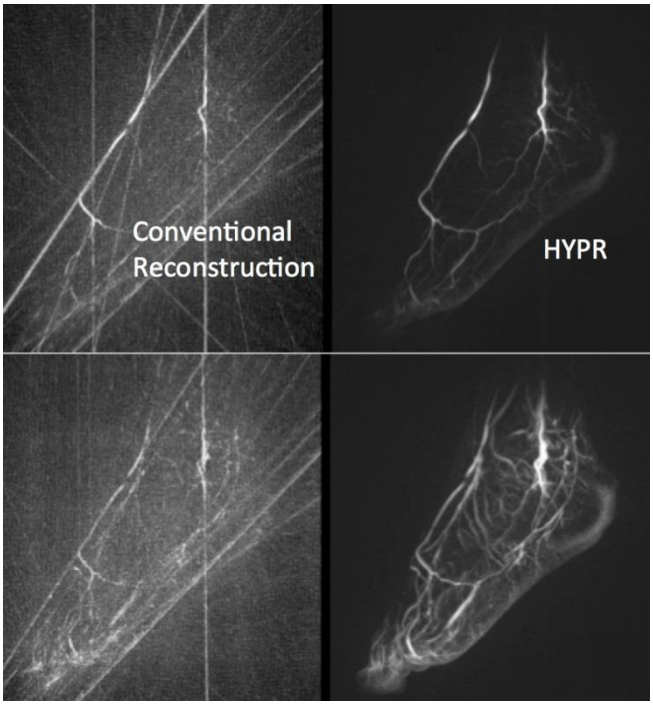

Figure 12. Comparison of conventional filtered back projection and HYPR reconstuction using a factor of 50 fewer than the Nyquist requirement. (Courtesu of Oliver Wieben).

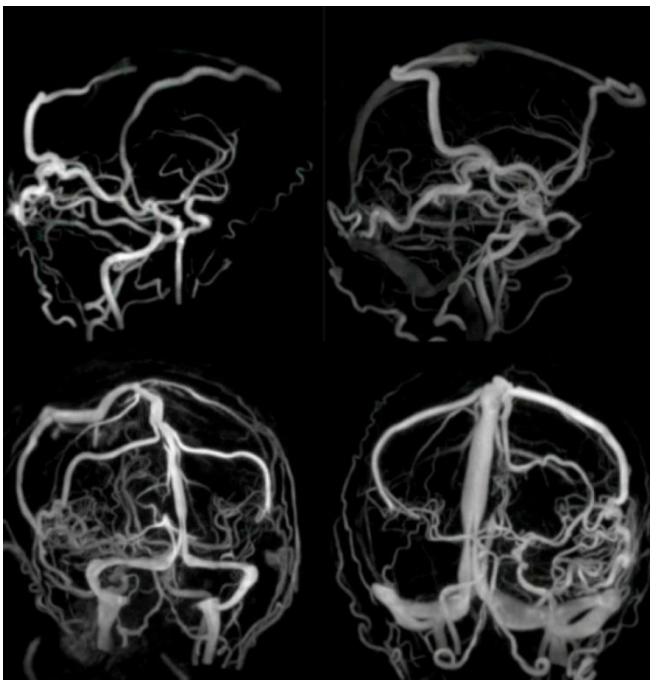

Figure 13. Hybrid HYPR VIPR MRA rotating time frames using an acceleration factor of 800 relative to conventional 3D radial Nyquist acquisition.

Figure 14 summarizes the MRA acceleration methods that have occurred since TRICKS.

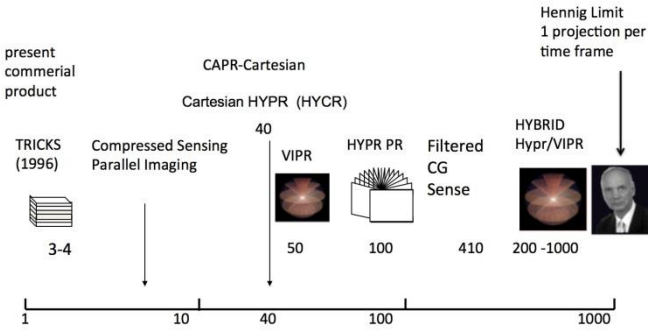

Figure 14. Acceleration Methods for Dynamic MRA

Ultimately, the optimal combination of all available techniques will move us closer to the Hennig limit of obtaining images with almost no data at all.

4D DSA

Commercial DSA systems have evolved from the original single plane projection systems to rotating C-arm systems that provide what is essentially a 3D CTA reconstruction of the vasculature providing a 3D DSA image which statically represents the average opacification of the vessels during the C-arm rotation [39,40]. The rotational 3D DSA image is traditionally acquired in an equilibrium phase in which all vessels are well opacified in all projections. This provides the optimal 3D reconstruction. However, we discovered that if inflow is permitted in the early stages of rotation, the 3D reconstruction can provide an adequate constraining image that can be used to help reconstruct time dependent information provided by each of the projections obtained during the rotation [41[. This ultimately provides 3D volumes at the projection frame rate, typically 15-30 fps. Assuming a ten second gantry rotation, this provides 300 rather than one 3D volume during the passage of the contrast. The result is a 4D DSA display in which arbitrary view angles can be used at any point in time and a time series that can be observed at any chosen angle. This greatly reduces the vascular overlap problems that were experienced in the earlty attempts to do intravenous DSA.

The basic idea is illustrated in Figure 15**.**

As indicated in Figure 15, once the 4D volumes have been reconstructed, any time frame can be viewed from arbitrary angles. This provides considerable flexibility in the study of the vasculature by providing views that may not be normally obtainable with the C-arm.

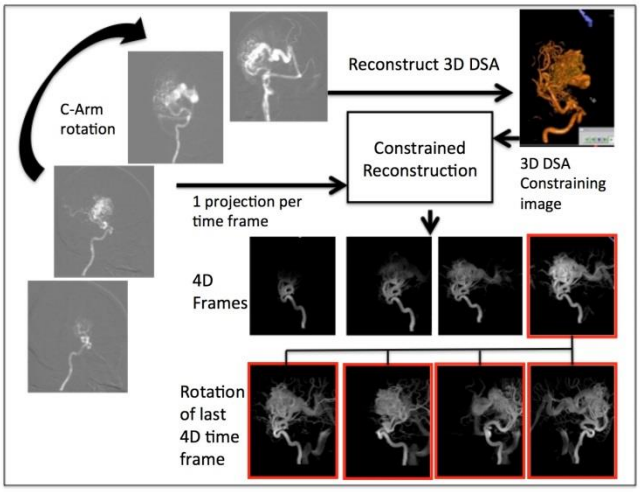

Figure 15. Schematic representation of 4D DSA

Figure 16 illustrates the effect of the constrained reconstruction on the SNR of the 4D DSA images. The image on the left is one of the acquired projections. This is compared with a corresponding 4D DSA frame (middle) and the 3D DSA constraining image (right).

Figure 17 shows MIPS through a series of 3D volumes in the case of an AVM. In this case each voxel has been colored to indicate the time of arrival of the contrast material. In addition to the temporal variations in the contrast intensity the color-coding provides quantitative information. It should be realized that although just two views are shown, any arbitrary view angle is available without additional gantry rotation. The view on the right represents a view in which the X-rays would have had to traverse from head to foot, a view not practical in a single 2D projection acquisition.

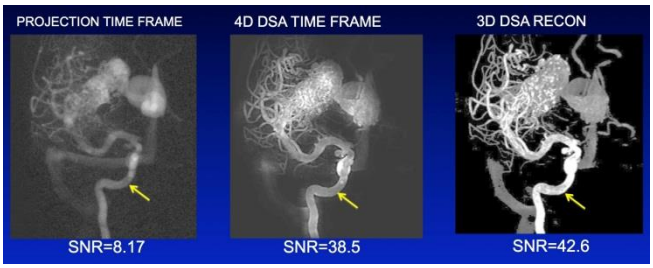

Figure 16. SNR comparison. Most of the SNR of the constraining image is transferred to the individual 4D DSA time frames so relative to the acquired projections, 4D DSA provides significantly higher SNR at all angles.

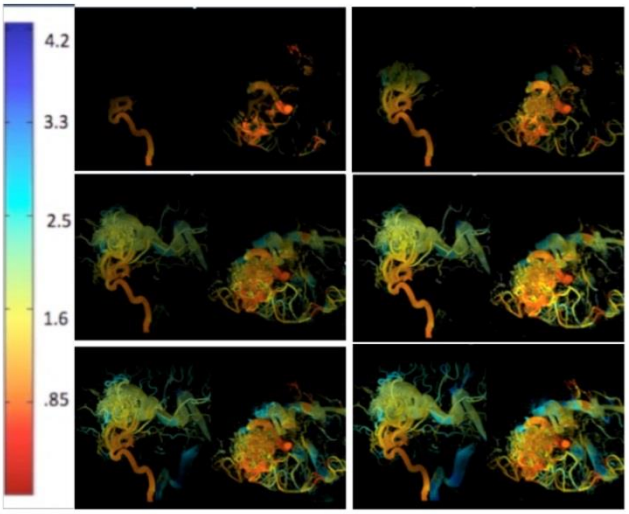

Figure 17. Time series of color coded 4D DSA time frames. The time series on the right is not obtainable using standard 2D acquisition techniques.

Figure 18 illustrates the simplification provided by 4D DSA in the evaluation of vessels following intravenous contrast injection. The 3D DSA volume (upper left) is complex and contains areteries and veins. The vessels of interest are easily seen in one of the arterial phase 4D DSA time frames (lower left). Twenty minutes were spent trying to see the vessels of interest by looking at cut planes (right) through the 3D DSA volume. The process was cumbursome and not very sucessful due to the fact that the vessels do not stay in discrete planes.

Figure 19 compares the temporal and spatial resolution of competing methods for time-resolved angiography. Conventional DSA has excellent temporal resolution but the voxel size is very large since displayed information is a projection through the whole volume. This has been demonstrated to produce lower contrast in small vessels compared with the MIP projections that can be used with 4D DSA.

Current MRA tehniques have significantly lower temporal resolution than 4D DSA although HYPR MRA does provide frame rates of 2-3 per second with sub-millimeter isotropic resolution.

CTA can provide frame rates of 2-3 per second with voxel sizes of about 0.1 mm^3. This is an order of magnitude slower than 4D DSA when images are constructed at 30 fps.

When 4D DSA volumes are reconstructed at 512^3 spatial resolution is comparable to CTA. However, the flat panel detectors used for 4D DSA have higher resolution than discrete CT detectors and can in principle support reconstrution at 1024^2, potentially providing an order of magnitude increase in spatial resolution relative to CTA.

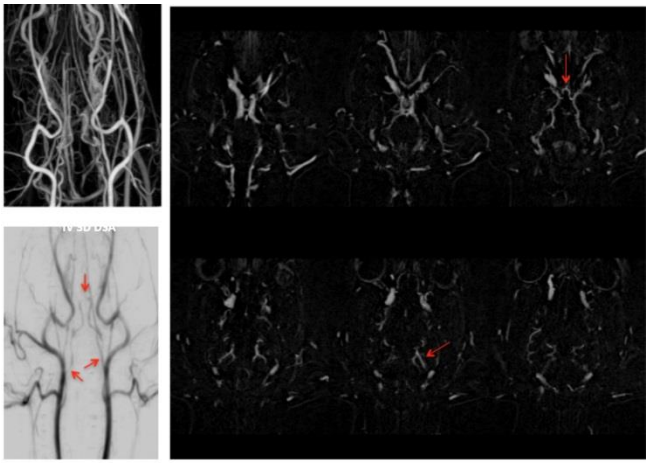

Figure 18. Comparison of vessel identifacation in 3D vs 4D DSA.

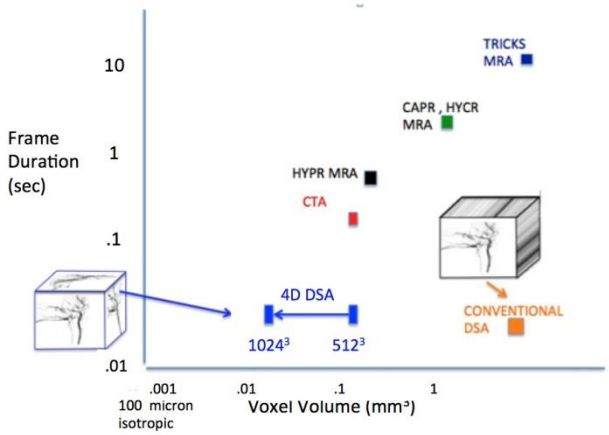

Figure 19. Spatial and temporal characteristics of competing time-resolved angiographic modalities,

Another significant difference beteeen CTA and 4D DSA, not shown in Figure 19, concerns the X-ray dose required for a dynamic series. In the case of 4D DSA all temporal frames are acquired with a single C-Arm rotation using a single X-ray dose. For a CTA time series containing 30 time frames, the dose would have to be repeated 30 times. Although the CTA data could eventually be subjected to something like HYPR processing which has been reported to reduce time resolved CT dose by perhaps 5, there remains an order of magnitude difference in the required dose for a time resolved 4D DSA exam and a time-resolved CTA exam.

So far 4D DSA has primarily been applied for neuroangiography where motion is minimal. For abdominal imaging, as was realized in the early days of DSA, there is a high probability of soft tissue artifacts. This was the motivation for the implementation of the hybrid energy/time method listed in Figure 2. We have simulated the expected image quality that would be generated by the third order tomographic energy/time term ($d^3I/dEdtdz$) which we call dual energy 4D DSA.

In the absence of energy switching capabilities on our C-arm system we performed two nearly identical injections and performed C-arm rotational acquisitions at 60 and 125 kVp. The projections from these two acquisitions were given weightings corresponding to soft tissue subtraction and were reconstructed using the standard 4D DSA algorithm. The results of this simulation are shown in Figure 20. Shown are the 4D DSA results at 60 kVp and 125 kVp, the tissue subtracted dual energy 4D DSA result and a series of selected 4D DSA time frames. The simulation does not test the tissue subtraction capabilities since there was no motion in the head. However, the SNR that remains after the tomographic energy/time subtraction is displayed in the time frames and appears to be adequate and certainly a large improvement over the SNR in Figure 9.

4D FLUOROSCOPY

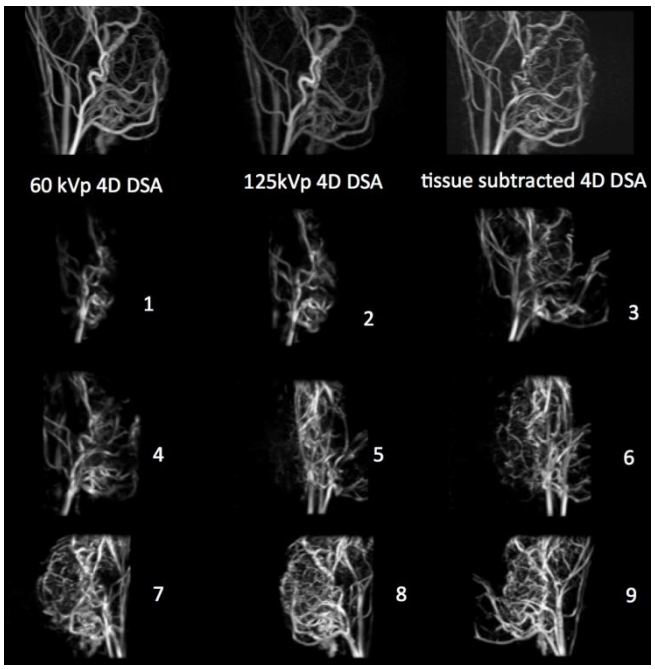

Figure 20. Simulation of dual energy 4D DSA.

During interventional procedures it is important to have an adequate view of the pathology and its relationship to the various interventional devices being employed. Even with bi-plane fluoroscopy it is sometimes not possible to acquire adequate views and the procedure is aborted and the patient is sent to surgery.

Using principles similar to those of 4D DSA we have been able to embed a 4D representation of the interventional device in the 3D space of the rotational DSA reconstruction and to view the device from arbitrary angles, including those normally unavailable, without gantry motion. So far this has been done retrospectively but will soon be available in real time. There is much validation that must still be done in terms of the accuracy of the representation of the device and means for dealing with potential motion. There is also additional algorithm development in progress to accommodate the many situations that arise during interventions such as the insertion of a coil into an aneursym already a containing a significant amount of coil.

The general idea of 4D fluoroscopy is shown in figure 21 where a coil is being inserted into an aneurysm. Shown are several points in time with one fixed angle and another rotating view. In practice the clinician could choose the optimal view angle from the 3D DSA study and then view the reconstructed 4D fluoro images at that angle. An endoscopic viewing mode is being developed and should assist with device placement when one of multiple intravascular openings must be chosen for device insertion.

DISCUSSION AND CONCLUSIONS

The evolution of DSA from the traditional method introduced in 1980 to the 4D version presented here has taken more thn 30 years. It has benefitted from the work done on the development of 3D DSA rotational angiography and the undersampled acquisition and constrained reonstruction principles learned in the course of developing accelerated MRA.

During our development of undersampled and constrained MRA tehniques there was much skepticism because our methods were consider intuitive, ad hoc and without mathematical justification. The extreme violations of the Nyquist theorem were a cause for considerable concern. However, shortly after our development of VIPR, Emmanuel Candes and colleagues from Cal Tech published what we consider to be a new Nyquist theorem [44,43] that proves that in the case of sparse data sets such as we have in angiography a good reconstruction of a image matrix with n^3 elements does not require n^3 data samples. Instead the required number is significantly less and depends on the number of non-zero voxels in the image volume. This theorem provides some insight into why the methods we had developed were successful.

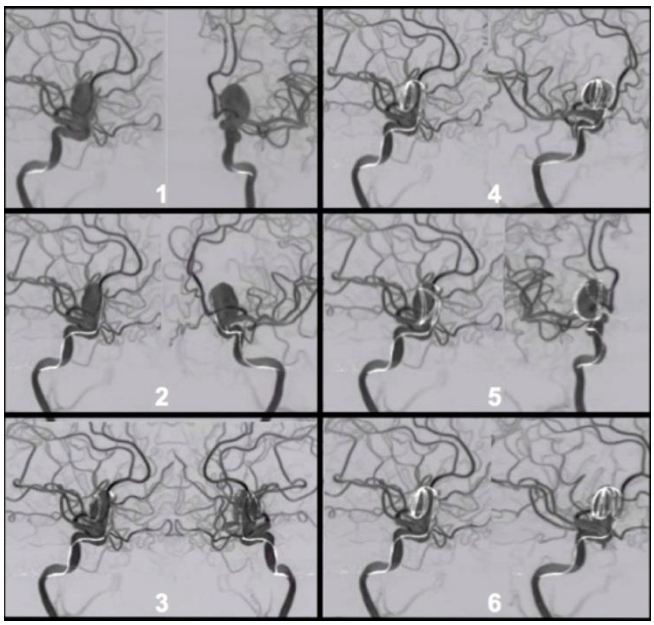

Figure 21. Demonstration of 4D fluoroscopy using retrospective processing of two bi-plane fluoroscopic views.

The use of undersampling and constrained reconstruction are likely to have implications in a broad range of medical imaging applications. The use of VIPR has enabled the development of ultrashort echo time imaging that provides a new means of imaging short T2* behavior [43] and has led to practical flow imaging in pediatric cardiology and other applications. Significant increases in SNR, reduced radiation dose and accelerated acquisition have been reported using HYPR processing in time-resolved CT [45-47], Photacoustic tomography [48], time resolved PET imaging [49,50], MR spectroscopy [51], and diffusion tensor imaging [52] There are now more advanced techniques than HYPR which incorporate iterative reconstruction and the methods generally associated with compressed sensing [53,54] These may provide some increase in the accelerations reported here.

The development of 4D DSA is an example of why it is useful to reexamine old techniques in view of new technology that has arisen. It is also important to look at advances in all imaging areas in order to seek tools that might be useful for any contemplated advance in any particular area. The development of 4D DSA made use of advances in CTA, MRA, and the general principles of undersampled acquisition and constrained imaging learned in the course of the development of ultrafast time-resolved MRA.

We would like to emphasize again that this arricle reflects the developments with which the author is most familiar. Any major advance in imaging depends heavily on the excellent body of work done by other investigators. In the case of DSA the introduction of digital electronic technology was a key factor. For the ultimate development of ultrafast time-resolved MRA, the introduction of gadolinium techniques [16], the development of techniques leading to the generation of high quality non-time-resolved scans [19,20], and prior work on constrained reconstruction [33,34] were important developments. Significant advances in MR hardware were contributed by industry. The development of 4D DSA relied heavily on the development of cone beam C-arm angiographic reconstruction [39,40].

It has been a privelege to work in the field of medical imaging for the past four decades. We believe that in the future medical imaging will continue to be an exciting and productive area of research.

ACKNOWLEDGEMENTS

In addition to the many graduate students including people like Robert Kruger and Stephen Riederer who worked with us during the development of DSA, we would like to acknowledge some of the radiologists who have played important roles in the development of the angiographic technques described in this paper. Dr. Joseph Sackett, Andrew Crummy, Charlie Strother and Pat Turski were key contributors to the original DSA technique. Dr. Strother is the co-inventor of 4D DSA and has provided both the inspiration for the technique and the expertise for its implementation into a clinically useable modality. Dr Tom Grist and Dr Turski have inspired the development of many time-resolved MRA methods.

We would like to acknowlege forty years of continuous funding, initially from NSF and then NIH. Our early DSA work was also supported by Phillips. All of the MRA work was supported in part by General Electric and the recent 4D DSA work has been done in collaboration with Siemens who have also contributed funding.

REFERENCES

1. Moniz E. (1927) L'encephalographie arteriale,son importance dans la localisation des tumeurs cerebrales. Rev Neurol 2:72-90.
2. Ziedses Des Plantes BG, (1934) "Planigraphieen subtractie. Roentgenographische differentiatie methoden thesis," Kemink en Zoon, Utrecht. p. 112.
3. Mistretta C.A (1974) The use of a general description of the radiological transmission image for categorizing imaging enhancement procedures. *Optical Engineering* 13(2):134.
4. Crummy AB, Mistretta CA, Ort MG, Kelcz F, Cameron JR, Siedband MP (1973) Absorption edge fluoroscopy using quasi-monoenergetic x-ray beams. *Investigative Radiology* 8:402-412.
5. Mistretta CA, Ort MG, Cameron JR, Crummy AB, Moran PR (1973) Multiple image subtraction technique for enhancing low contrast periodic objects. *Investigative Radiology* 8:43-49.
6. Ducos de Lahitte M, Marc-Vergnes JP, Rascol A, Guiraud B, and Manelfe C (1980) Intravenous angiography of the extracranial cereral arteries, Radiology 137:3 705-711.
7. Ovitt TW et al. (1979) "Development of a digital subtraction system for intravenous angiography," Proc. SPIE, 206, 183–189.
8. Brennecke R et al. (1977) "Computerized video-image preprocessing with applications to cardio-angiographic roentgen-image series," in Digital Image Processing, H. H Nagel (Springer-Verlag, Berlin), 244–262.
9. Mistretta CA, Kruger RA, Houk TL, Riederer SJ, Shaw CG, Ergun DL, Kubal W, Crummy AB, Zwiebel W, Rowe G, Zarnstorff W, Flemming D (1978) Computerized fluoroscopy techniques for noninvasive cardiovascular imaging. SPIE, *Appl Opt Instr Med*, 152:65-71
10. Kruger RA, Mistretta CA, Lancaster J, Houk TL, Goodsitt MM, Riederer SJ, Hicks J, Sackett JF, Crummy AB, Flemming D (1978) A digital video image processor for real-time subtraction imaging. *Optical Engineering* 17(6):652-657.
11. Kruger RA, Mistretta CA, Riederer SJ, Ergun DL, Shaw CG, Rowe GG (1979) Computerized fluoroscopy techniques for noninvasive imaging of the cardiovascular system. *Radiology* 130(1): 49-57.
12. Strother CM, Sackett JF, Crummy AB, Lilleas FG, Zwiebel W, Turnipseed W, Javid M, Mistretta CA, Kruger RA, Ergun DL, Shaw CG (1980), Clinical applications of computerized fluoroscopy: the extracranial carotid artery. *Radiology* 136(3):781-783.
13. Crummy AB, Strother CM, Sackett JF, Ergun DL, Shaw CG, Kruger RA, Mistretta CA, Turnipseed WD, Lieberman RP, Myerowitz PD, Ruzicka FF (1980) Computerized fluoroscopy: a digital subtraction technique for intravenous angiocardiography and arteriography. *AJR* 135:1131-1140.
14. Waugh JR and Sacharias N (1992), Arteriographic complications in the DSA era, Radiology 182, 243–246.
15. Brody WR, (1981) Hybrid subtraction for improved arteriography, Radiology141(3), 828–831.
16. Prince MR, Yucel EK, Kaufman JA, Harrison DC, Geller SC (1993) Dynamic gadolinium enhanced three dimensional abdominal MR arteriography. J Magn Reson Imaging 3:877-881.
17. Lee VS, Martin DJ, Krinsky GA, Rofsky NM. (2000) Gadolinium enhanced MR angiography, artifacts and pitfalls. AJR Am J Roentgenol 175:197–205.
18. Foo TK, Saranathan M, Prince MR, Chenevert TL (1997) Automated detection of bolus arrival and initiation of data acquisition in fast, three-dimensional, gadoliniumenhanced MR angiography. Radiology 203:275-280.
19. Wilman AH, Riederer SJ, King BF, Debbins JP, Rossman PJ, Ehman RL(1997) Fluoroscopically triggered contrast-enhanced three dimensional MR angiography with elliptical centric view order:application to the renal arteries. Radiology 205:137–146.
20. Riederer SJ, Fain SB, Kruger DG, Busse RF (1999) Real-time imaging and triggering of 3D contrast-enhanced MR angiograms using MR fluoroscopy. MAGMA 8:196–206.
21. Van Vaals J, Brummer ME, Dixon WT, et al. (1993) Keyhole method for accelerating imaging of contrast agent uptake. J Magn Reson Imaging 3:671–675.
22. Doyle M, Walsh EG, Blackwell GG, Pohost GM (1995) Block Regional Interpolation Scheme for k-Space (BRISK): A Rapid Cardiac Imaging Technique, Magnetic Resonance in Medicine, 33.163-170.
23. Mistretta CA, Grist TM, Frayne R, Korosec F, and Polzin JA (1995) Simulation and Implementation of a Breath-Hold Method for Time-Resolved 3D Contrast Imaging, Proceedings of the International Society of Magnetic Resonance Annual Meeting, New York, NY.
24. Korosec FR, Frayne R, Grist TM, Mistretta CA (1996) Time-resolved contrast-enhanced 3D MR angiography. *Magn Reson Med* 36:345-351.
25. Scheffler K and Hennig J (1998) Reduced circular field of view imaging, Magn. Reson. Med. 40, 474–480 .
26. Peters DC., Grist TM, Korosec FR, Holden JE, Block WF, Wedding KL, Carroll TJ, Mistretta CA (2000) Undersampled projection reconstruction applied to MR angiography," Magn. Reson. Med. 43(1), 91–101.
27. Barger AV, Block WF, Toropov Y, Grist TM, Mistretta CA (2002) Time-resolved contrast-enhanced imaging with isotropic resolution and broad coverage using an undersampled 3D projection trajectory. *Magn Reson Med* 48: 297-305.
28. Turk AS, Johnson KM, Lum D, Niemann D, Aagaard-Kienitz B, Consigny D, Grinde J, Turski P, Haughton V, Mistretta CA (2007) Physiological and anatomic assessment of a canine artery stenosis model with phase contrast with vastly undersampled isotropic projection imaging, AJNR Am. J. Neuroradiol. 28: 111 - 115.
29. Moftakhar R, Aagaard-Kienitz B, Johnson KM, Turski PA, Consigny D, Grinde J, Turk AS, Niemann DB, Mistretta CA (2007) Non-invasive measurement of intra-aneurysmal pressure and flow velocity using phase contrast vastly undersampled projection imaging (PC VIPR), *AJNR;* 28(9):1710-4.
30. Lum DP, Johnson KM, Paul RK, Turk AS, Consigny DW, Grinde JR, Mistretta CA and Grist TM (2007), Measurement of Trans-stenotic Pressure Gradients in Swine Comparison Between Retrospective ECG-Gated 3D Phase-Contrast MRA and Endovascular Pressure-Sensing Guidewires. Radiology 245: 751-760.
31. Bley TA, Johnson KM, Francois CJ, Reeder SB, Schiebler ML, Consigny D, Grist TM, and Wieben O (2011) Noninvasive assessment of transstenotic pressure gradients in porcine renal artery stenoses by using vastly undersampled phase-contrast MR angiography, Radiology, vol. 261, no. 1, pp. 266-73.
32. Francois CJ, Srinivasan S, Schiebler ML, Reeder SB, Niespodzany E, Landgraf BR, Wieben O, Frydrychowicz A (2012) 4D cardiovascular magnetic resonance velocity mapping of alterations of right heart flow patterns and main pulmonary artery hemodynamics in tetralogy of Fallot, J Cardiovasc Magn Reson, 14: 1, pp. 16.
33. Webb AG, Liang ZP, Magin RI, and Lauterbur PC (1993) Applications of reduced encoding MR imaging with generalized series reconstruction (RIGR), J. Magn. Reson. Imaging 3(6), 925–928.
34. Tsao J, Boesiger P, and Pruessmann KP, k-t BLAST and k-t SENSE: Dynamic MRI with high frame rate exploiting spatiotemporal correlations, Magn. Reson. Med. 50(5), 1031–1042.
35. Mistretta CA, Wieben O, Velikina J, Block W, Perry J, Wu Y, Johnson K, Wu Y (2006) Highly constrained backprojection for time-resolved MRI, *Magn Reson Med* 55: 30-40.
36. Johnson KM, Velikina J, Wu Yijing, Kecskemeti S, Wieben O, and Mistretta CA (2008) Improved Waveform fidelity Using Local

HYPR Reconstruction (HYPR LR), *Magn Reson Med.* Volume 59, Issue 3,:456-462.
37. Wu Y (2011), Time Resolved Contrast Enhanced Intracranial MRA using a single dose delivered as sequential injections and Highly Constrained Projection Reconstruction (HYPR CE), Magn Reson Med., published online: 17 FEB 2011 | ,DOI: 10.1002/mrm.22792.
38. Haider CR, Borisch EA, Glockner JF, Mostardi PM, Rossman PJ, Young PM, Riederer SJ (2010) Max CAPR: high-resolution 3D contrast-enhanced MR angiography with acquisition times under 5 seconds. *Magn Reson Med*. 64(4):1171-81.
39. Ning R and Kruger RA (1998) Computer simulation of image intensifier basedCTdetector: Vascular application," Med. Phys. 15(2), 188–192.
40. Fahrig R, Ganguly A, Starman J, and Strobel N (2004) C-arm CT with XRIIs and digital flat panels: A review, SPIE 49th Annual Meeting, Denver, Colorado, 5535.
41. Davis B, Strother CM, Mistretta CA et al. (2013) 4D DSA: Implementation and Demonstration of Feasibility, Accepted for publication in AJNR.
42. Candès E, Romberg J, Velikina J, Ron A, Mistretta CA (2004) Image reconstruction from highly undersampled data using total variation minimization. International Workshop on MR Angiography, London Ontario, 2004.
43. Candes EJ, Romberg J, and Tao T, (2006) Robust uncertainty principles:. Exact signal reconstruction from highly incomplete frequency information, IEEE Trans. Inf. Theory 52(2), 489–509.
44. Takahashi AM, Lu A, Brittain JH, Hinks RS, Shimakawa A, Johnson JW, Cunningham CH, W. F. Block WF, Pauly JM, Bydder GM (2005) Ultra Short TE (UTE) Imaging at 8 μsec with 3D Vastly Undersampled Isotropic Projection Reconstruction (VIPR), Proc. Intl. Soc. Mag. Reson. Med. 13.
45. Supanich M, Tao Y, Nett B, Pulfer K, Hsieh J, Turski P, Mistretta CA, Rowley H, Chen GH (2009) Radiation Dose Reduction in Time-Resolved CT Angiography Using Highly Constrained Back Projection Reconstruction , Phys. Med. Biol. 54 4575.
46. Liu X, Primak AN, Krier JD, Yu L, Lerman LO, and McCollough CH (2008) Accurate, in vivo determination of renal perfusion and hemodynamics using HYPR noise reduction and a ten-fold decrease in radiation dose, Abstract, *RSNA* (2008).
47. Krissak R, Mistretta CA, Henzler T, Chatzikonstantinou A, Scharf J, et al. (2011) Noise Reduction and Image Quality Improvement of Low Dose and Ultra Low Dose Brain Perfusion CT by HYPR-LR Processing. PLoS ONE 6(2): e17098.doi:10.1371/journal.pone.0017098
48. Kruder R, Reinecke D, Kruger G, Thornton M, Picot P, Morgan T, Stantz K, Mistretta CA(2009) HYPR-spectral photoacoustic CT for preclinical imaging,Proc. SPIE 7177, Photons Plus Ultrasound: Imaging and Sensing , 71770F ; doi:10.1117/12.810175.
49. Christian BT, Vandehey NT, Floberg J, Mistretta CA (2010) Dynamic PET denoising with HYPR Processing. *J Nucl Med* 51: 7 1147-1154.
50. Floberg JM, Holden JE, Weichert JP, Hall LT, Mistretta CA, and Christian BT(2012) Improved kinetic Analysis of Dynamic [C-11]PIB Data with Optimized HYPR-LR, Med. Phys. **39**, 3319.
51. Wang K, Du J, O'Halloran R, Fain, Kecskemeti SS, Wieben O, Johnson KM, Mistretta, CA (2009) Ultrashort TE Spectroscopic Imaging Using Complex HYPR LR Reconstruction, Magn Reson Med. 62(1):127-34.
52. Alexander A, Lee J, Mistretta CA (2006) Diffusion Tensor Imaging with HighlY constrained backPRojection (HYPR), Abstract 858, International Society for Magnetic Resonance in Medicine.
53. Lee GR, Seiberlich N, Sunshine JL, Carroll TJ, Griswold MA (2013) Rapid time-resolved magnetic resonance angiography via a multiecho radial trajectory and and GraDeS reconstruction. Magnetic Resonance in Medicine, Volume 69:2 346–359.
54. Chen GH, Tang J, Leng S (2008) Prior image constrained compressed sensing (PICCS): a method to accurately reconstruct dynamic CT images from highly undersampled projection data sets, Med Phys. 35(2):660-663.

Corresponding author:
Author: Charles A Mistretta
Institute: The University of Wisconsin-Madison
Country: USA
Email: camistre@wisc.edu